Application of differential geometry in agricultural vehicle dynamics

J. Rédl, V. Váliková

Department of Machine Design, Faculty of Engineering, Slovak University of Agriculture in Nitra, Nitra, Slovak Republic

Abstract

Rédl J., Váliková V., 2013. **Application of differential geometry in agricultural vehicle dynamics**. Res. Agr. Eng., *59* (Special Issue): S34–S41.

This paper deals with the application of differential geometry methods to a precise calculation of the length of trajectory of an agricultural mechanism that moves on a sloping terrain. We obtained technical exciting function from experimental measurements, out of which we obtained the function of Euler's parameters by using computer processing. The processing of these parameters provided translational and angular velocities of the gravity centre of the systemic vehicle MT8-222, which performed the determined mounted manoeuvres. We obtained differential equations that describe the function of a spatial curve by the application of differential geometry methods. The length of the curve is obtained by a numerical solution of the differential equations formed. We used Dormand-Prince numerical method for the numerical solution. Next, we evaluated the error of the numerical integration for every calculation by reason of the stability of computation. We also addressed the geometric characteristics of the curves such as the radius of curvature. The mounted manoeuvres as well as the corresponding velocities, trajectories, and radiuses of curvature were processed in a graphic way.

Keywords: trajectory modelling; numerical integration; radius of curvature

The analysis, planning, and optimisation of the vehicle trajectory are nowadays intensively examined problems not only in the field of the agricultural mechanisms movement in relation to precision agriculture but also in the modelling and simulation of the vehicle motion and in the research into the dynamic effects on the vehicle. The research into the trajectory of the vehicle motion focuses also on the fields of development and design of the set mechanisms capable of autonomous decision and generation of the trajectory according to the input values from the sensors. Such a design is preceded by a simulation process which is based on differential moving equations of a rigid body as well as of a system of rigid bodies. Euler's parameters are used for the spatial dislocation of the vehicle and spatial transformation based on orthogonal matrices as well as the principles of differential geometry. To define the tire – ground relationship, the principles of terramechanics are advantageously used. An intensive research is realised also in the fields of the analysis of the vehicle trajectory in different reference coordinate axes, when the dynamics of transport is investigated as introduced in Punzo et al. (2011). They point out the possibility of obtaining the exact vehicle trajectory with the help of GPS or using the simulation programme NGSIM (Next Generation SIMulation; Federal Highway Administration, Washington DC, USA). It is possible to obtain precise values of the trajectory length by utilisation of GPS data, but a high risk exists of the loss of signal in mountain-

ous areas. Purwin and D'Andrea (2006) dealt with the generation and planning of the vehicle trajectory to provide its exact motion and minimise its trajectory to the accurately specified destination. The analysis of the stability of motion and the compliance of the specified trajectory of the vehicle motion are processed in the works of Ailona et al. (2005) and Yoon et al. (2009). Yoon et al. (2009) designed a dynamic model for the generation of the vehicle trajectory following the properties of the terrain and dislocation of a terrain barrier where there it is not possible to pass through it. Antos and Ambrósio (2004) presented strategies of the control of vehicle motion pursuant to the dynamics of rigid bodies. They realised simulations in the environment of the program Matlab® (MathWorks, Natick, USA). For spatial transformations, Euler's parameters were used advantageously. The result was the design of a driver which is able to provide vehicle motion according to the trajectory generated before. Under the authority of the differential geometry, model and real trajectories were evaluated. Almost in every work, the trajectory was generated by dynamic equations that had been generalised by Pacejka (2005).

MATERIAL AND METHODS

The length of the curve. Šalát (1981) as well as Ivan (1989) describes the length of the curve by means of differential geometry in the identical way. Parameterisation of the curve is addressed also by Agoston (2005).

Let K be a curve, which is defined by parameterisation:

$$\boldsymbol{r} = \boldsymbol{r}(t);\ t \in \langle \alpha, \beta \rangle \quad (1)$$

where:

$\boldsymbol{r}$ – denomination of function for parameterisation

$\boldsymbol{r}(t)$ – parameterisation of curve K in point t

α, β – initial and end point of the curve

Denote $\boldsymbol{R}(\alpha) = A$, $\boldsymbol{R}(\beta) = B$. The point A is the original point and point B is the final one of the curve K when its orientation is induced by parameterisation. Let $D = \{t_0, t_1, t_2, \dots, t_r\}$, where $\alpha < t_0 < t_1 < t_2 \dots < t_r = \beta$ is a certain division of the interval <α, β>.

where:

$\boldsymbol{R}(\alpha)$ – parameterisation of curve K in point α

$\boldsymbol{R}(\beta)$ – parameterisation of curve K in point β

D – set of points, which divides interval <α, β> into r-divisions

t_0–t_r – r-divisions of interval <α, β>

Denote $M_i = \boldsymbol{R}(t)$, for $i = 0, 1, 2, \dots, r$. Points $M_0, M_1, \dots, M_r$ follow gradually one after another in the orientation of the curve accordant with parameterisation (1), thus:

$$A = M_0 < M_1 < M_2 < \dots < M_r = B \quad (2)$$

These points divide the curve K into r partial curves (arcs) $\widehat{M_{i-1}M_i}$. We substitute each of them by an abscissa (subtense) $M_{i-1}M_i$. We denote the broken line consisting of abscissas $M_{i-1}M_i$ ($i = 1, 2, \dots, r$) as $K(D)$. We say that the broken line $K(D)$ is inscribed into the curve K.

Let's (D) denote the length of the broken line K(D). Hence:

$$s(D) = \sum_{i=1}^{r} d(M_{i-1}, M_i) = \sum_{i=1}^{r} |r(t_i) - r(t_{i-1})| \quad (3)$$

where:

d – length of the partial curves

It can happen (if the curve is not simple) that the point M_{i-1} is identical with the point M_i for some i. In this case, it holds that $d(M_{i-1}, M_i) = 0$.

Using the foregoing way, every division D of the interval <α, β> is assigned a positive number $s(D)$, which presents the length of the corresponding inscribed break line $K(D)$. To every sequence $\{D_n\}$ of the division of the interval <α, β> appertains the sequence of number $\{s(D_n)\}$. It is evident that, if there exists a number, that $d(D_n) \leq s$ for every division D_n and the lower the difference $d(D_n) \leq$ s the smoother the division D, then the non-negative number s is called the length of the curve K. We establish a definition:

If the corresponding sequence $\{s, D_n\}$ for every regular sequence $\{D_n\}$ of the division of the interval <α, β> is convergent and the limit does not depend on the selection of sequence $\{D_n\}$, we say that the curve K is rectifiable and we name the number $s = \lim_{n\to\alpha} s(D_n)$ its length.

According to this definition and knowledge of the transformation of the parameter of the curve, it can be relatively easy to prove that the length of the curve does not depend on its parameterisation. From the geometric point of view, it is an obvious requirement for the definition of the curve length.

From the definition of the curve length and theorems about the limit of numeric sequence follows the veracity of the next theorem.

Theorem 1 (monotony property)

If the curve K is rectifiable and its length is s, then its each part K' is rectifiable too and for its length s′ holds: $s \leq s'$.

By the help of this theorem, the theorem about other important property of the curve length (additive property) can be proved.

Theorem 2 (additive property)

(a) If the curve K is rectifiable, then for its optional division into the final number of partial curves K_1, K_2, … , K_n each from parts K_1 is rectifiable and it holds:

$$s = s_1 + s_2 + \ldots + s_i + \ldots + s_n \tag{4}$$

where:

s – length of the curve K

s_i – length of its parts K_i, i = 1, 2, … n

(b) The curve K, which is the connection of the final number of rectifiable curves K_1, K_2, …, K_n, is also rectifiable and for its length s holds the equality (4).

The following theorem speaks out about a sufficient condition of the curve rectifiability.

Theorem 3

Let $\boldsymbol{r} = \boldsymbol{r}(t)$, $t \in \langle\alpha, \beta\rangle$ be parameterisation of the curve K. If the function $\boldsymbol{r}$ has a continuous derivative $\boldsymbol{r}'$ in the interval $\langle\alpha, \beta\rangle$ (in the point A from the right, in the point B from the left), then the curve K is rectifiable and for its length s holds:

$$s = \int_{\alpha}^{\beta} \left|\frac{dr(t)}{dt(t)}\right| dt \tag{5}$$

that is:

$$s = \int_{\alpha}^{\beta} \sqrt{\left[\frac{dx(t)}{dt}\right]^2 + \left[\frac{dy(t)}{dt}\right]^2 + \left[\frac{dz(t)}{dt}\right]^2}\, dt \tag{6}$$

$$\text{if } \boldsymbol{r}(t) = x(t)\mathbf{i} + y(t)\mathbf{j} + z(t)\mathbf{k} \tag{7}$$

where:

i, **j**, **k** – unity vectors

x, y, z – coordinates

This corollary follows from the definition of the regular and partly regular curves and from theorems 2 and 3.

When we utilise the parameterisation of the curve K, we obtain a flexion of the curve. For the regular curve K holds that for every point the flexion equals:

$$\varkappa = \sqrt{[x''(t)]^2 + [y''(t)]^2 + [z''(t)]^2} \tag{8}$$

Using Eq. (7) and its first and second derivation leads to the relation for the curvature of the curve. We establish determinants A, B, C as:

$$\mathrm{A} = \begin{vmatrix} y', & z' \\ y'', & z'' \end{vmatrix}, \mathrm{B} = \begin{vmatrix} z', & x' \\ z'', & x'' \end{vmatrix}, \mathrm{C} = \begin{vmatrix} x, & y' \\ x'', & y'' \end{vmatrix} \tag{9}$$

For the curvature in every point of the curve K then holds:

$$\mathrm{K} = \frac{\sqrt{\mathrm{A}^2 + \mathrm{B}^2 + \mathrm{C}^2}}{\sqrt{[(x(t)')^2 + (y(t)')^2 + (z(t)')^2]^3}} \tag{10}$$

From the preceding relations we can define the radius of curvature as the reciprocal of the curvature:

$$\rho = \frac{1}{\mathrm{K}} \tag{11}$$

Numerical integration. In the created application, the numerical method is implemented for integration of Runge-Kutta methods, especially Dormand-Prince method. This method is analysed in the paper of its authors Dormand and Prince (1980). They presented this method thanks to Butcher's table, in which the coefficients of the individual terms in the equations are described. Butcher's table was used also by Hoppensteadt (2007). The equations for Dormand-Prince method have the following forms:

$$k_1 = h_n f(x_n, y_n)$$

$$k_2 = h_n f\left(x_n + \frac{1}{5}h_n, y_n + \frac{1}{5}k_1\right)$$

$$k_3 = h_n f\left(x_n + \frac{3}{10}h_n, y_n + \frac{3}{40}k_1 + \frac{9}{40}k_2\right)$$

$$k_4 = h_n f\left(x_n + \frac{4}{5}h_n, y_n + \frac{44}{45}k_1 - \frac{56}{15}k_2 + \frac{32}{9}k_3\right)$$

$$k_5 = h_n f\left(x_n + \frac{8}{9}h_n, y_n + \frac{19{,}372}{6{,}561}k_1 - \frac{25{,}360}{2{,}187}k_2 + \frac{64{,}448}{6{,}561}k_3 - \frac{212}{729}k_4\right)$$

$$k_6 = h_n f\left(x_n + h_n, y_n + \frac{9{,}017}{3{,}168}k_1 - \frac{355}{33}k_2 - \frac{46{,}732}{5{,}247}k_3 + \frac{492}{176}k_4 - \frac{5{,}103}{18{,}656}k_5\right) \tag{12}$$

$$k_7 = h_n f\left(x_n + h_n, y_n + \frac{35}{384}k_1 - \frac{500}{1{,}113}k_3 + \frac{125}{192}k_4 - \frac{2{,}187}{6{,}784}k_5 + \frac{11}{84}k_6\right)$$

$$y_{n+1} = y_n + \frac{35}{284}k_1 + \frac{500}{1{,}113}k_3 + \frac{125}{192}k_4 - \frac{2{,}187}{6{,}784}k_5 + \frac{11}{84}k_6$$

where:
k_1–k_7 – Runge-Kutta koefficients
h_n – step of the numerical integration
y_n, y_{n+1} –the value in the points x_n, x_{n+1}

Quaternion feedback control. Wie (2008) considers the attitude dynamics of a rigid vehicle described by Euler's rotational equation of the motion:

$$\mathbf{J}\dot{\boldsymbol{\omega}} + \boldsymbol{\omega} \times \mathbf{J}\boldsymbol{\omega} = \mathbf{u} \tag{13}$$

where:
$\mathbf{J}$ – inertia matrix
$\boldsymbol{\omega} = (\omega_1, \omega_2, \omega_3)$ – angular velocity vector
$\mathbf{u} = (u_1, u_2, u_3,)$ – control torque input vector

The cross product of two vectors is represented in the matrix notation as

$$\boldsymbol{\omega} \times \mathbf{h} = \begin{bmatrix} 0 & -\omega_3 & \omega_2 \\ \omega_3 & 0 & -\omega_1 \\ -\omega_2 & \omega_1 & 0 \end{bmatrix} \begin{bmatrix} h_1 \\ h_2 \\ h_3 \end{bmatrix} \tag{14}$$

where:
$\mathbf{h} = \mathbf{J}\boldsymbol{\omega}$ – angular momentum vector

It is assumed that the angular velocity vector components ω_i along the body/fixed control axes are measured by rate gyros.

Euler's rotational theorem states that the rigid body attitude can be changed from any given orientation to any other orientation by rotating the body around an axis, called the Euler axis, which is fixed to the rigid body and is stationary in inertial space. Such a rigid body rotation around the Euler axis is often called the eigenaxis rotation.

Let a unit vector along the Euler axis be denoted by $\mathbf{e} = (e_1, e_2, e_3)$, where e_1, e_2 and e_3 are direction cosines of the Euler axis relative to either an inertial reference frame or the body – fixed control axes. The four elements of quaternions (q_1–q_4) are then defined as:

$$\begin{aligned} q_1 &= e_1 \sin(\theta/2) \\ q_2 &= e_2 \sin(\theta/2) \\ q_3 &= e_3 \sin(\theta/2) \\ q_4 &= \cos(\theta/2) \end{aligned} \tag{15}$$

where:
θ – denotes the rotation angle around the Euler axis

and we have:

$$q_1^2 + q_2^2 + q_3^2 + q_4^2 = 1 \tag{16}$$

The quaternion kinematic differential equations are given by:

$$\begin{bmatrix} \dot{q}_1 \\ \dot{q}_2 \\ \dot{q}_3 \\ \dot{q}_4 \end{bmatrix} = \frac{1}{2} \begin{bmatrix} 0 & \omega_3 & -\omega_2 & \omega_1 \\ -\omega_3 & 0 & \omega_1 & \omega_2 \\ \omega_2 & -\omega_1 & 0 & \omega_3 \\ -\omega_1 & -\omega_2 & -\omega_3 & 0 \end{bmatrix} \begin{bmatrix} q_1 \\ q_2 \\ q_3 \\ q_4 \end{bmatrix} \tag{17}$$

Like the Euler-axis vector $\mathbf{e} = (e_1, e_2, e_2)$, defining a quaternion vector $\mathbf{q} = (q_1, q_2, q_2)$ as:

$$\mathbf{q} = \boldsymbol{e} \sin(\theta/2) \tag{18}$$

we rewrite Eq. (17) as

$$\begin{aligned} 2\dot{\mathbf{q}} &= q_4\boldsymbol{\omega} - \boldsymbol{\omega} \times \mathbf{q} \\ 2\dot{q} &= -\boldsymbol{\omega}^T\mathbf{q} \end{aligned} \tag{19}$$

where:

$$\boldsymbol{\omega} \times \mathbf{q} = \begin{bmatrix} 0 & -\omega_3 & \omega_2 \\ \omega_3 & 0 & -\omega_1 \\ -\omega_2 & \omega_1 & 0 \end{bmatrix} \begin{bmatrix} q_1 \\ q_2 \\ q_3 \end{bmatrix} \tag{20}$$

Because quaternions are well-suited for on-board real-time computation, the vehicle orientation is nowadays commonly described in terms of quaternions, and a linear state feedback controller of the following form can be considered for real-time implementation:

$$\boldsymbol{u} = -\boldsymbol{K}\mathbf{q_e} - \boldsymbol{C}\boldsymbol{\omega} \tag{21}$$

where $\mathbf{q_e} = (q_{1e}, q_{2e}, q_{3e})$ is the attitude error quaternion vector and $\mathbf{K}$ and $\mathbf{C}$ are controller gain matrices to be properly determined. The attitude error quaternions (q_{1e}, q_{2e}, q_{3e}, q_{4e}) are computed using the desired or commanded attitude quaternions (q_{1c}, q_{2c}, q_{3c}, q_{4c}) and the current attitude quaternions (q_1, q_2, q_3, q_4) as follows:

$$\begin{bmatrix} q_{1e} \\ q_{2e} \\ q_{3e} \\ q_{4e} \end{bmatrix} = \begin{bmatrix} q_{4c} & q_{3c} & -q_{2c} & -q_{1c} \\ -q_{3c} & q_{4c} & q_{1c} & -q_{4c} \\ q_{2c} & -q_{1c} & q_{4c} & -q_{3c} \\ q_{1c} & q_{2c} & q_{3c} & q_{4c} \end{bmatrix} \begin{bmatrix} q_1 \\ q_2 \\ q_3 \\ q_4 \end{bmatrix} \tag{22}$$

If the commanded attitude quaternion vector is simply the origin defined as

$$(q_{1c}, q_{2c}, q_{3c}, q_{4c}) = (0, 0, 0, +1) \tag{23}$$

then the control logic (21) becomes:

$$\boldsymbol{u} = -\boldsymbol{K}\mathbf{q} - \boldsymbol{C}\boldsymbol{\omega} \tag{24}$$

On the other hand, if the origin is chosen as (0, 0, 0, –1), then the control logic (21) becomes:

$$\boldsymbol{u} = +\boldsymbol{K}\mathbf{q} - \boldsymbol{C}\boldsymbol{\omega} \tag{25}$$

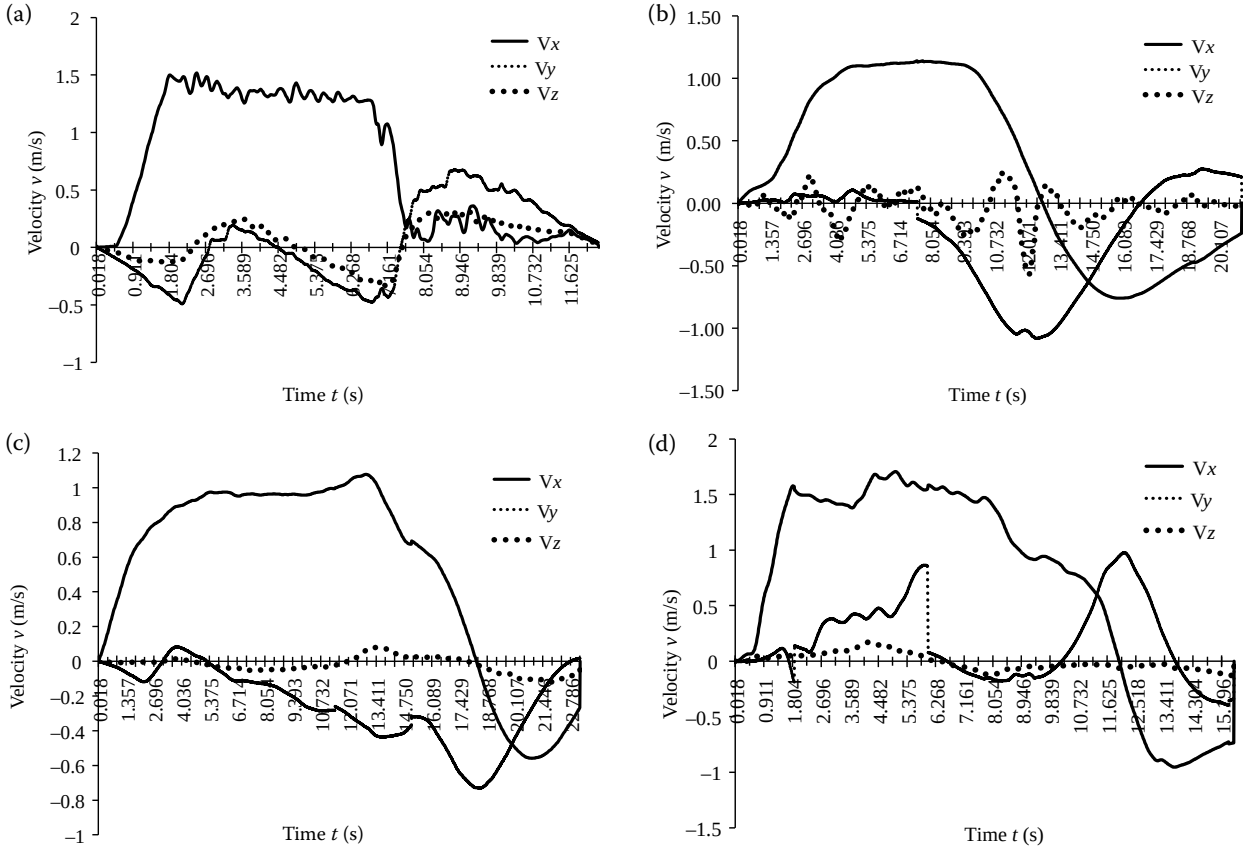

Fig. 1. Translational velocities of the centre of gravity: (a) Manoeuvre 1, (b) Manoeuvre 2, (c) Manoeuvre 3, (d) Manoeuvre 4
V*x*, V*y*, V*z* – velocities in the direction of *x*, *y*, *z* axis, respectively

Agricultural machine and determination of manoeuvres. The agricultural machine used in these experiments was the systemic vehicle MT8-222 (ZTS Obchodný podnik, Slovenská Ľupča, Slovak Republic) that is designated for working on the sloping terrain. The design of this machine is addressed by Páltik et al. (2007). The average value of the slope gradient was 30–33 degrees. Experimental measurements were done from which we got the functions of the acceleration of the centre of gravity. When we processed these functions with a computer, we obtained Euler's parameters. The processing of these parameters yielded the translational and angular velocities of the centre of gravity of the systemic vehicle MT8-222, which performed the determined mounted manoeuvres. The moments of inertia of the vehicle with respect to the *x*, *y*, *z* axes were J_x = 240 kg.m^2, J_y = 520 kg.m^2, and J_z = 950 kg.m^2. The weight of the vehicle was 1.356 kg.

Four different manoeuvres were executed:

Manoeuvre 1: moving on the slope along the down-grade slope with braking.

Manoeuvre 2: moving on the slope along the down-grade slope with turning to the down-grade slope.

Manoeuvre 3: moving on the slope along the hillside with turning to the hillside.

Manoeuvre 4: moving on the slope along the down-grade slope with 45 degree yaw angle with turning to the down-grade slope.

The real trajectories executed during the manoeuvres are shown below. We assume that all of the discreet functions used by us were in the given interval <0, *t*>, where *t* is the time of the manoeuvre execution, continuous. We suppose the existence of the position vector of the vehicle centre of gravity towards the origin of inertial coordinate system in every instant of time. During the manoeuvres execution, there was no overturn of the vehicle.

We respected the standard SAE J670 200801 (1976) as for the terminology of the vehicle dynamics.

RESULTS AND DISCUSSION

We recommend for use in practice that curves, obtained by this approach, were approximate by polynomial functions owing to the achievement of better smoothness of the function continuance,

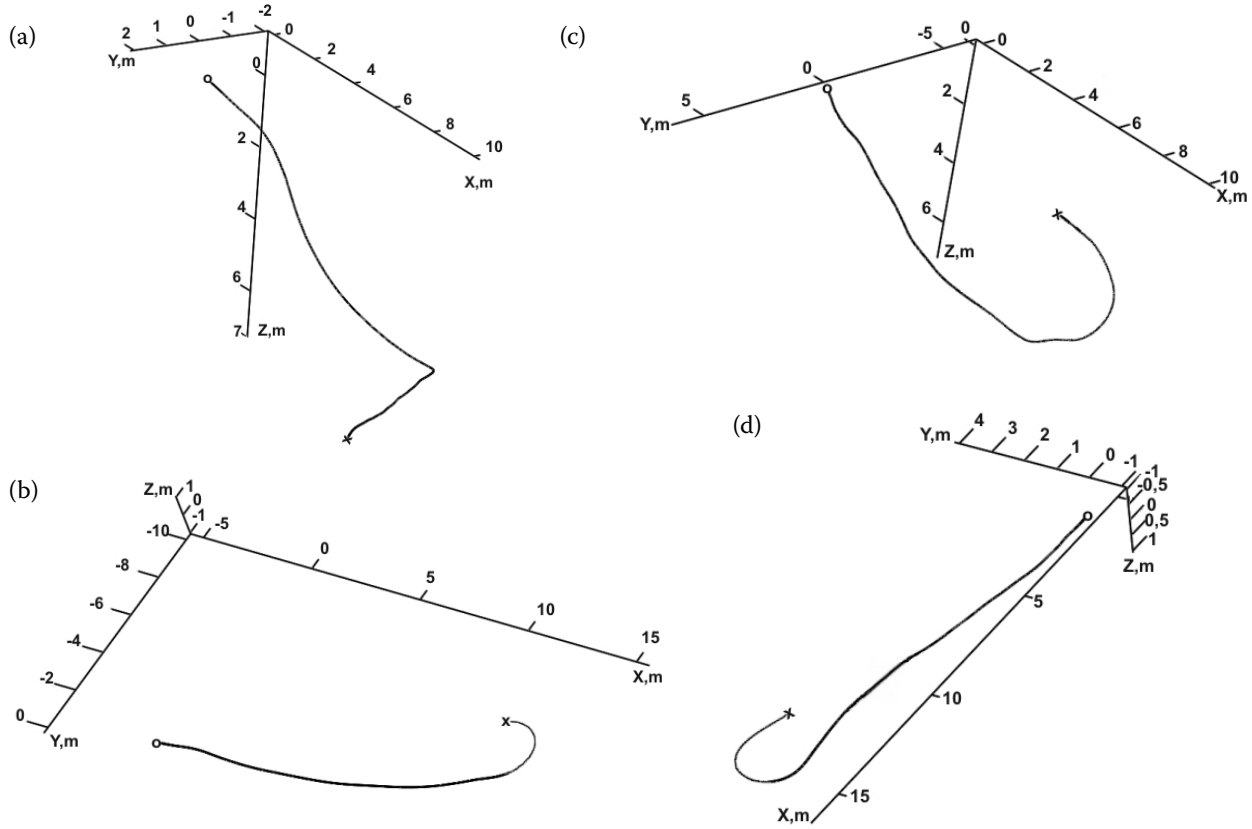

Fig. 2. Vehicle manoeuvres: (a) Manoeuvre 1; (b) Manoeuvre 2; (c) Manoeuvre 3; (d) Manoeuvre 4

whereas our functions have a stochastic character. The algorithm we formed uses also characteristic parameters of the curve such as flexion, torsion, and curvature, but their exposure would surpass the size of this contribution. That is why we present only the radius of curvature ρ. We substitute the values of translational accelerations, velocities, and the dislocations of the centre of gravity into the corresponding parameters in Eqs (6), (7), (9) and (10). The coordinates of the centre of gravity towards the inertial reference frame were obtained by utilisation of Eq. (16) to (25), similarly to Šesták et al. (1993) and Schaub et al. (2002). Using Eq. (16), we determined the stability of the evaluation of Euler's parameters and also the error of the evaluation, which was in the range of 3.10^{-13}–4.10^{-13}. To solve the system of simultaneous differential equations (Eq. 17), we used Dormand-Prince method in the form of Eq. (12) for the computation of Euler's parameters. By means of Euler's parameters, we created the transformation matrix in the form:

$$[M_T]_i = \prod_{i=1}^{n} \begin{bmatrix} q_1^2 + q_2^2 - q_3^2 - q_4^2 & 2(q_2q_3 + q_1q_4) & 2(q_2q_3 - q_1q_3) \\ 2(q_2q_3 - q_1q_4) & q_1^2 + q_3^2 - q_4^2 - q_2^2 & 2(q_3q_4 + q_1q_2) \\ 2(q_4q_2 + q_1q_3) & 2(q_3q_4 - q_1q_2) & q_1^2 + q_4^2 - q_2^2 - q_3^2 \end{bmatrix}_i^T \quad (26)$$

whereas in every i-cycle the matrix is transposed. The components of the vectors of the translational and angular velocities of the centre of gravity in the inertial system were determined from the transformation equations as follows:

$$\begin{bmatrix} v_{XE} \\ v_{YE} \\ v_{ZE} \end{bmatrix}_i = \begin{bmatrix} M_T \end{bmatrix}_i \times \begin{bmatrix} \frac{dx(t)}{dt} \\ \frac{dy(t)}{dt} \\ \frac{dz(t)}{dt} \end{bmatrix}_i, \begin{bmatrix} \omega_{XE} \\ \omega_{YE} \\ \omega_{ZE} \end{bmatrix} = \begin{bmatrix} M_T \end{bmatrix}_i \times \begin{bmatrix} \frac{d\theta_x(t)}{dt} \\ \frac{d\theta_y(t)}{dt} \\ \frac{d\theta_z(t)}{dt} \end{bmatrix}_i \quad (27)$$

In Fig. 1, the translational velocities are shown for Manoeuvres 1, 2, 3, and 4.

The coordinates of the centre of gravity in the inertial system were obtained by integration:

$$\begin{bmatrix} x_E \\ y_E \\ z_E \end{bmatrix}_i = \int_0^t \begin{bmatrix} v_{XE} \\ v_{YE} \\ v_{ZE} \end{bmatrix}_i dt \quad (28)$$

Table 1. The lengths of the trajectories for Manoeuvres 1, 2, 3, and 4

Manoeuvre	Trajectory (s, m)	Error of numerical integration
1	11.076	–8.515E-14
2	17.996	–4.689E-13
3	18.744	–4.026E-13
4	18.169	–1.197E-12

Real trajectories of Manoeuvres 1, 2, 3, and 4 were obtained by solving Eq. (28) and are shown in Fig. 2.

To obtain the length of each trajectory of Manoeuvres 1, 2, 3, and 4, we used Eq. (6). The application of the methods of differential geometry gives us differential equations that describe the function of the spatial curve, in this case the trajectory. To solve these differential equations, we used the application created in the Delphi development environment. This application implements the numerical method Dormand-Prince (Eq. 12) and enables us to obtain the results of differential equations by numerical integration. The results achieved are given in Table 1. Also listed are the errors of numerical integration for each evaluation of the length of the vehicle trajectory.

According to Eq. (11), we evaluated the values of the radius of curvature for each manoeuvre. Fig. 3 shows the continuances of the radiuses of curvature for Manoeuvres 1 to 4. Due to limpidity, we reduced the number of the displayed points in Manoeuvres 1 and 2 in Fig 3a, b. We used the logarithmic scale to display the graphs. For the evaluation of parameters in Eqs (8), (9), and (10), we substitute x, y, z, x′, y′, z′, x″, y″, z″ by x_E, y_E, z_E, v_{xE}, v_{yE}, v_{zE}, a_{xE}, a_{yE}, a_{zE}, respectively.

As shown in Fig. 3, the shapes of the curves have a stochastic continuance. From the realised simulation computation it follows that the acceleration function has a deforming influence on the continuance of the radius of curvature. It is possible to obtain a smoother continuance of the acceleration functions by reverse derivation, but we do not recommend it because of a high inaccuracy. The results of the length of trajectory obtained by the approach mentioned seem highly evidentiary in comparison with the real experiment.

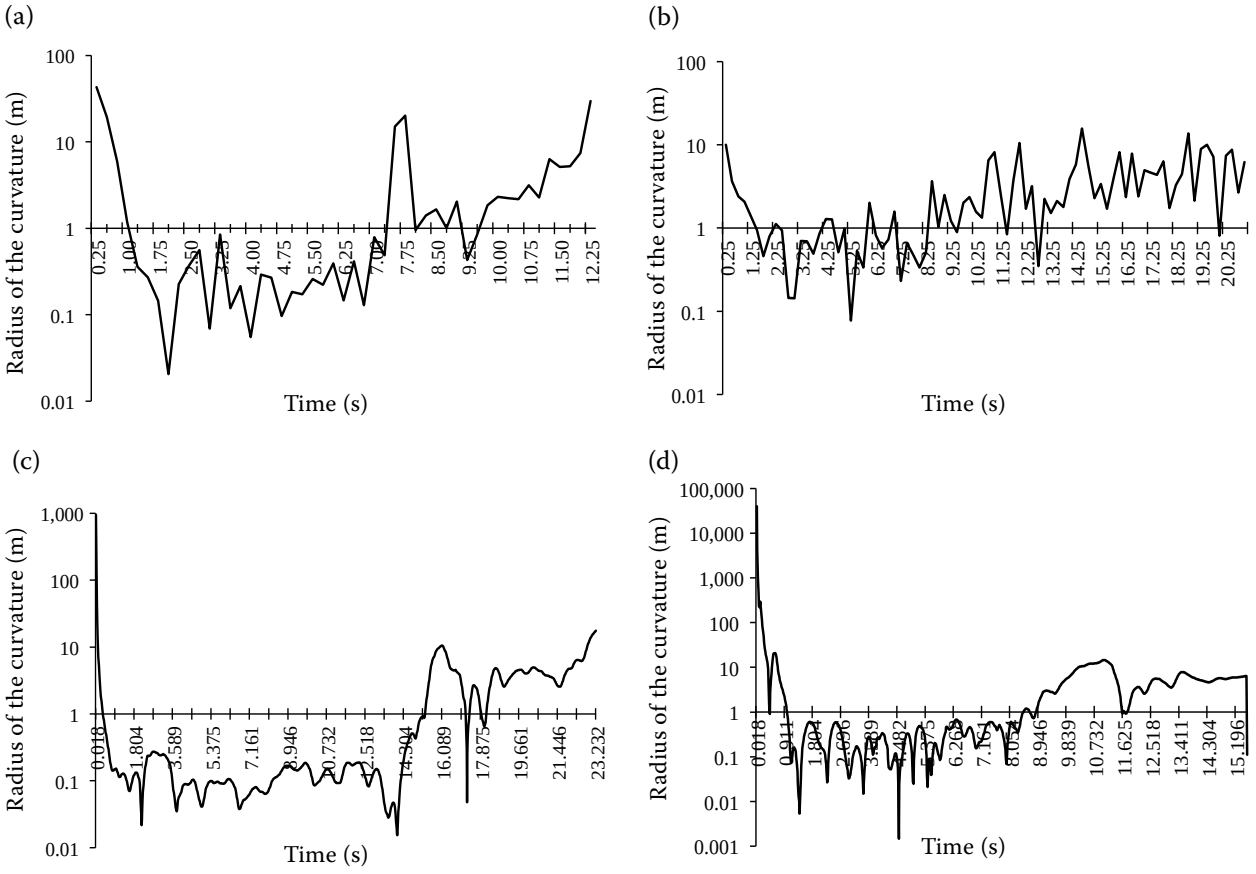

Fig. 3. Radius of curvature of the vehicle trajectory: (a) Manoeuvre 1; (b) Manoeuvre 2; (c) Manoeuvre 3; (d) Manoeuvre 4

CONCLUSION

In this contribution, we addressed the application of differential geometry in the determination of the trajectory followed by the systemic vehicle MT8-222 in executing four different manoeuvres on the sloping terrain. We also dealt with the evaluation of the radius of curvature for each manoeuvre. The length of the trajectory was 11.076 m for Manoeuvre 1, 17.996 m for Manoeuvre 2, 18.744 m for Manoeuvre 3, and 18.169 m for Manoeuvre 4. The radiuses of curvature for each manoeuvre are interpreted in a graphic way. The described methodology using Euler's parameters has been published also by Šesták et al. (1993), as well as by Schaub et al. (2002), Rédl (2007), and Wie (2008). The stability of the numerical integration was provided by the determination of the error of the numerical integration. The step of the numerical integration was determined as h_n = 1/56, which corresponds with the experimental measurement on the agricultural machine. The methods and approaches presented are utilisable in the case of the determination of the specified trajectory and required manoeuvres of automatic mobile devices in the field of precision agriculture, as well as in the modelling and simulation of the vehicle motion or in the research into dynamic effects on the vehicle.

References

Agoston M.K., 2005. Computer Graphics and Geometric Modeling. London, Springer-Verlag: 959.

Ailona A., Berman N., Arogeti S., 2005. On controllability and trajectory tracking of a kinematic vehicle model. Automatica, *41*: 889–896.

Antos P., Ambrósio J.A.C., 2004. A control strategy for vehicle trajectory tracking using multibody models. Multibody System Dynamics, *11*: 365–394.

Dormand J.R., Prince P.J., 1980. A family of embedded Runge-Kutta formulae. Journal of Computational and Applied Mathematics, *6*: 19–26.

Hoppensteadt F.C., Jackiewicz Z., Zubik–Kowal B., 2007. Numerical solution of volterra integral and integro – differential equations with rapidly vanishing convolution kernels. BIT Numerical Mathematics, *47*: 325–350.

Ivan J., 1989. Matematika 2. [Mathematics 2.] Bratislava, Alfa: 632.

Pacejka H.B., 2005. Tire and Vehicle Dynamics, 2nd Ed. SAE International: 642.

Páltik J., Findura P., Maga J., Korenko M., Angelovič M., 2007. Poľnohospodárske stroje. [Agricultural Machines.] Nitra, Slovak University of Agriculture in Nitra: 190.

Punzo V., Borzacchiello M.T., Ciuffo B., 2011. On the assessment of vehicle trajectory data accuracy and application to the Next Generation SIMulation (NGSIM) program data. Transportation Research Part C, *19*: 1243–1262.

Purwin O., D'Andrea R., 2006. Trajectory generation and control for four wheeled omnidirectional vehicles. Robotics and Autonomous Systems, *54*: 13–22.

Rédl J., Kročko V., 2007. Analýza stability výpočtu Euler – Rodriguesových parametrov. [Solving stability analysis of Euler – Rodrigues parameters.] Acta Facultatis Technicae, *11*: 125–133.

SAE J670 2008-01, 2008. Vehicle Dynamics Terminology. Warrendale, SAE International.

Šalát T., 1981. Malá encyklopédia matematiky. [Little Encyclopedia of Mathematics.] 3rd Ed. Bratislava, Obzor: 856.

Šesták J., Sklenka P., Škulavík L., 1993. Matematické modely terénnych vozidiel určené na popis ich správania pri práci na svahu. [Mathematical Models of Terrain Vehicles Designated for Description of the Behaviour When Operating on the Slope.] Nitra, VES VŠP: 91.

Schaub H., Junkins J.L., 2002. Analytical Mechanics of Space Systems. Virginia, American Institute of Aeronautics and Astronautics: 558.

Wie B., 2008. Space Vehicle Dynamics and Control. 2nd Ed. Virginia, American Institute of Aeronautics and Astronautics: 985.

Yoon Y., Shin J., JinKim H., Park Y, Sastry S., 2009. Model – predictive active steering and obstacle avoidance for autonomous ground vehicles. Control Engineering Practice, *17*: 741–750.

Received for publication July 3, 2012
Accepted after corrections January 31, 2013

Corresponding author:

doc. Ing. Jozef Rédl, Ph.D., Slovak University of Agriculture in Nitra, Faculty of Engineering, Department of Machine Design, Tr. A. Hlinku 2, 949 76 Nitra, Slovak Republic
phone: + 421 376 415 670, e-mail: redl@is.uniag.sk